

# Generation of dual-wavelength pulses by frequency doubling with quasi-phase-matching gratings

G. Imeshev and M. M. Fejer

*E. L. Ginzton Laboratory, Stanford University, Stanford, California 94305*

A. Galvanauskas and D. Harter

*IMRA America, 1044 Woodridge Anenue, Ann Arbor, Michigan 48105*

Received September 20, 2000

We demonstrate generation of two synchronized picosecond pulses at different wavelengths near 778 nm by frequency doubling of a femtosecond pulse. We use nonlinear frequency filtering with quasi-phase-matching gratings, which allow us to obtain second-harmonic spectral intensities that are higher than the spectral intensities of the pump. © 2001 Optical Society of America

OCIS codes: 140.7090, 190.7110, 190.2620, 320.5540, 320.7110.

Synchronized short pulses generated at two different wavelengths are required in such applications as pump-probe experiments, coherent control, and generation of short pulses in the mid infrared by difference-frequency generation. Over the past several years a number of dual-wavelength Ti:sapphire oscillators have been demonstrated that use relatively complex dual-cavity designs to eliminate timing jitter between the pulses.<sup>1-4</sup> Another approach to the generation of dual-wavelength pulses is to use linear frequency filtering of a single pulse.<sup>5,6</sup>

The utility of longitudinally nonuniform quasi-phase-matching (QPM) gratings for fairly arbitrary pulse shaping by second-harmonic generation (SHG) has been demonstrated.<sup>7,8</sup> This technique combines pulse shaping with SHG in compact and monolithic devices and relies on the engineerability of the QPM gratings. A QPM grating acts as a filter on the frequency components of the first-harmonic (FH) pulse; this QPM SHG filter function is proportional to the Fourier transform of the spatial distribution of the nonlinear coefficient.<sup>9,10</sup>

Here we use this QPM SHG pulse-shaping technique to demonstrate generation of synchronized dual-wavelength pulses. Using structures with a phase-reversal sequence superimposed upon a uniform grating, we produce two synchronized coherent picosecond pulses by QPM SHG spectral filtering of a single femtosecond FH pulse. The wavelengths of the second-harmonic (SH) pulses and their temporal lengths are determined by the grating design, subject to limitation by the bandwidth of the FH pulse. Because of the nonlinear nature of QPM SHG filtering, the energy efficiency is not limited by the passband of the filter and, in fact, the SH spectral intensity can exceed the FH spectral intensity over the same bandwidth. We note that QPM devices similar to those described here have already been used for a cw frequency conversion.<sup>11</sup>

Under the assumptions of plane-wave interaction, an undepleted pump, slowly varying envelopes, and negligible group velocity and higher-order dispersion of the material, the QPM SHG process is described with a transfer-function relation<sup>9,10</sup>:

$$\hat{A}_2(\Omega) = \hat{D}(\Omega)\widehat{A}_1^2(\Omega), \quad (1)$$

where  $\hat{A}_2(\Omega)$  is the frequency-domain envelope of the output SH and  $\widehat{A}_1^2(\Omega)$  is the self-convolution of the frequency-domain envelope of the input FH and hence is proportional to the spectrum of the nonlinear drive. In Eq. (1),  $\hat{D}(\Omega)$  is the QPM SHG transfer function, which is proportional to the Fourier transform of the nonlinear coefficient distribution  $d(z)$ :

$$\hat{D}(\Omega) = -i\gamma \int_{-\infty}^{+\infty} d(z)\exp[-i(\Delta k_0 + \delta v\Omega)z]dz, \quad (2)$$

where  $\gamma \equiv 2\pi/\lambda_1 n_2$ ,  $\lambda_1$  is the FH wavelength, and  $n_2$  is the SH refractive index. In Eq. (2)  $\Delta k_0 = 2k_1 - k_2$  and  $\delta v = 1/u_1 - 1/u_2$ , where  $k_i$  are the carrier  $k$  vectors and  $u_i = (dk/d\omega)^{-1}|_{\omega=\omega_i}$  are the group velocities for the FH ( $i = 1$ ) and the SH ( $i = 2$ ).

We first consider a constant-duty-cycle uniform QPM grating of length  $L$  and period  $\Lambda_0$  (and hence the grating  $k$  vector for first-order QPM  $K_0 = 2\pi/\Lambda_0$ ). Ultrashort-pulse SHG with such gratings was previously analyzed in the literature<sup>10,12,13</sup>; we reproduce those results here for reference. The QPM SHG transfer function  $\hat{D}_0(\Omega)$  for such a grating is calculated with Eq. (2) as

$$\hat{D}_0(\Omega) = \gamma L |d| \text{sinc}(\delta v\Omega L/2), \quad (3)$$

where  $|d|$  is related to the intrinsic nonlinear coefficient of the material,  $d_{\text{eff}}$ , as  $|d| = (2/\pi)d_{\text{eff}}$  for first-order QPM; we also assume that the QPM condition is satisfied:  $K_0 = \Delta k_0$ . Equation (3) gives a familiar  $\text{sinc}^2$  tuning curve when  $|\hat{D}_0(\Omega)|^2$  is evaluated. The tuning curve is centered at  $\Omega = 0$  and has a FWHM of  $\Delta\Omega_0 = 5.57/(\delta vL)$ , which, for a given  $\delta v$  (material parameter), is determined by the grating length. If the width of  $\hat{D}_0(\Omega)$  is much smaller than the bandwidth of the nonlinear drive  $\widehat{A}_1^2(\Omega)$ ,  $\Delta\Omega$ , the spectrum of the generated SH essentially replicates  $\hat{D}_0(\Omega)$ ; hence in the time domain the SH is a long (compared with the FH) top-hat pulse of length  $\delta vL$  [see Fig. 1(a)], as is well known from the literature.<sup>14</sup>

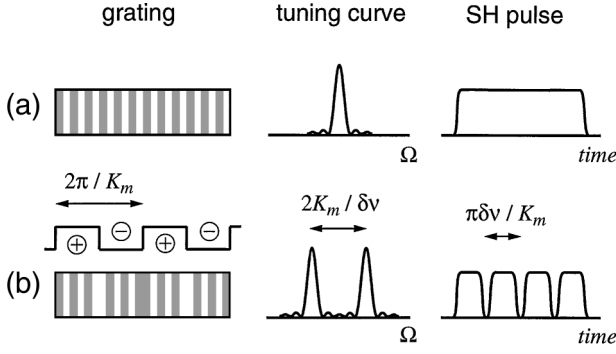


Fig. 1. Schematic of the QPM SHG nonlinear filtering devices.

We now consider a QPM grating in which a periodic phase reversal sequence of period  $\Lambda_m$  is superimposed upon the nonlinear coefficient distribution of the uniform grating [Fig. 1(b)]. This modulation  $\Pi(z)$  is represented by the Fourier series as

$$\Pi(z) = \sum_{n=1,3,\dots} (2/\pi n) [\exp(inK_m z) + \exp(-inK_m z)], \quad (4)$$

where  $K_m = 2\pi/\Lambda_m$  is the  $k$  vector of the modulation. The QPM SHG transfer function is then calculated with Eq. (2) as

$$\hat{D}_m(\Omega) = \sum_{n=1,3,\dots} (2/\pi n) [\hat{D}_0(\Omega - n\Omega_m) + \hat{D}_0(\Omega + n\Omega_m)], \quad (5)$$

where  $\Omega_m = K_m/\delta v$ . As can be seen, the effect of modulation  $\Pi(z)$  on the transfer function is splitting of the single spectral peak, as is well known from Fourier analysis:  $\hat{D}_m(\Omega)$  has a series of peaks at frequencies  $\Omega = \pm n\Omega_m$ , whose amplitudes scale as  $1/n$ . For further analysis we neglect the contribution of higher-order terms (with  $n \geq 3$ ) to Eq. (5) because the two terms with  $n = 1$  contain  $\approx 81\%$  of the total spectral power of  $\hat{D}_m(\Omega)$ ; the contribution of the higher-order terms to the SH spectrum is further diminished if  $\Omega_m$  is comparable with the bandwidth of the nonlinear drive and can be further reduced with apodized grating designs. We further assume that the spectral variations of the nonlinear drive over the bandwidths of  $\hat{D}_0(\Omega \pm \Omega_m)$  are small, which for pulses with smooth spectra leads to the condition that the width of the individual peaks of transfer function  $\Delta\Omega_0$  is much smaller than drive bandwidth  $\Delta\Omega$ . If the splitting between the peaks,  $2\Omega_m$ , is of the order of  $\Delta\Omega$ , this condition is equivalent to  $\Lambda_m \ll L$ . Under these assumptions we obtain the output SH pulse envelope, using Eqs. (1) and (5), as

$$\hat{A}_2(\Omega) = (2/\pi) [\hat{A}_1^2(\Omega = \Omega_m) \hat{D}_0(\Omega - \Omega_m) + \hat{A}_1^2(\Omega = -\Omega_m) \hat{D}_0(\Omega + \Omega_m)]. \quad (6)$$

The result of Eq. (6) can be interpreted as the spectrum of two coherent long (compared with the FH pulse) SH pulses of lengths  $\delta v L$  with different center frequencies.

We note that filtering of frequency components with such a QPM grating can be viewed as a simple rejection of the nonlinear drive frequencies outside the desired narrow spectral bands. However, the important distinction between a linear bandpass filter and the nonlinear QPM SHG filtering action is the efficiency of the filtering process. By the nature of the linear bandpass filter the energy in the filtered pulse scales with the bandwidth of the filter, and hence almost all the pulse energy will be rejected by a narrow-band filter. In contrast, for the QPM SHG filter the efficiency is nearly independent of the filtering bandwidth. Such a QPM SHG filter can produce spectral intensities that are comparable with or even higher than that at the FH, because SH frequency component  $\Omega$  is generated not only from the  $\Omega$  component of the FH pulse but also from pairs of components  $\Omega'$  and  $\Omega - \Omega'$  for all  $\Omega'$  within the bandwidth of the FH pulse.

This insensitivity of the QPM SHG filter efficiency to the filter bandwidth (which is inversely proportional to grating length  $L$ ) is described formally in terms of the area under the tuning curve,  $|\hat{D}(\Omega)|^2$ , which is proportional to  $L$  but does not depend on the details of the nonlinear coefficient distribution as long as the grating does not contain unmodulated (no QPM grating) sections.<sup>10</sup> In the case of confocal focusing, for a fixed energy and pulse length the peak intensity of the FH pulse is inversely proportional to  $L$ . Together, these scalings make the energy efficiency independent of  $L$  and hence independent of the filtering bandwidth.

To put these scaling considerations into more-quantitative terms, we calculate the energy efficiencies for the QPM SHG devices considered in this Letter by following the procedure described in Ref. 10. We use the result of Eq. (6) and integrate the SH spectral intensity over all frequencies, assuming confocal focusing and a Gaussian FH pulse with  $1/e$  intensity half-width  $\tau_1$ . The efficiency is then obtained as

$$\eta = (8/\pi^2) \exp[-(1/2)\tau_1^2 \Omega_m^2] \eta_0, \quad (7)$$

where  $\eta_0$  is the efficiency for the uniform grating whose transfer function is given by Eq. (3). For SHG of a FH at wavelength of  $1.56 \mu\text{m}$  in a QPM grating fabricated upon a lithium niobate substrate,  $\eta_0 = 265\%/nJ U_1$ , where  $U_1$  is the FH pulse energy.<sup>10</sup> The numerical prefactor in Eq. (7) is less than unity because we neglected the contribution of the higher-order terms to the transfer function given by Eq. (5).

To demonstrate generation of dual-wavelength pulses we fabricated three devices, each of length  $L = 40 \text{ mm}$ , with different modulation periods upon a single chip by electric-field poling of a 0.5-mm-thick lithium niobate wafer.<sup>15</sup> QPM period  $\Lambda_0$  was  $18.7 \mu\text{m}$ , and the chip was held at  $150^\circ\text{C}$ . The pump source was an amplified Er: fiber laser producing pulses at  $1556 \text{ nm}$  with an energy of  $2.4 \text{ nJ}$ , a pulse length of  $570 \text{ fs}$ , and a bandwidth of  $8 \text{ nm}$ . The laser output was loosely focused through the chip into a spot size of  $120 \mu\text{m}$ .

Device (a) was a uniform grating with no phase-reversal modulation. The triangular shape of the SH

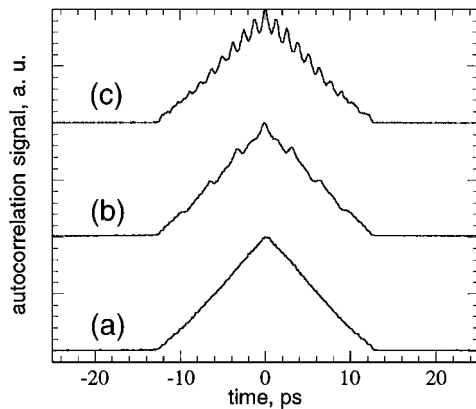


Fig. 2. SH autocorrelation traces for devices (a)–(c).

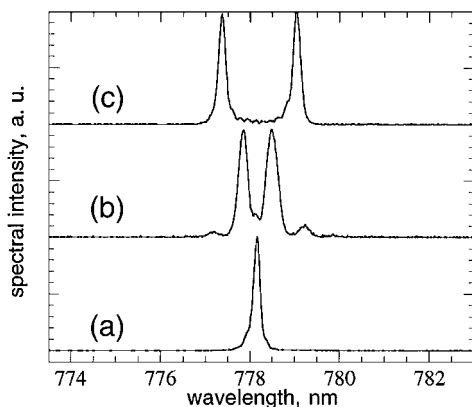


Fig. 3. SH spectra of the picosecond pulses obtained with devices (a)–(c).

autocorrelation trace [Fig. 2, curve (a)], implies a top-hat profile of the pulse itself. Its FWHM of 12.1 ps agrees well with the expected pulse length of  $\delta vL = 12.4$  ps. The SH spectrum [Fig. 3, curve (a)], is a single peak with a width of 0.18 nm. Slight peak broadening, compared with the expected value of 0.14 nm, is due to the finite instrumental resolution (0.05 nm) of the spectrum analyzer.

Devices (b) and (c) had modulation periods of  $\Lambda_m = 0.5L = 20$  mm and  $\Lambda_m = 0.2L = 8$  mm, respectively. The spectra [Fig. 3, curves (b) and (c)], consist of two peaks with a separation of 0.62 nm for device (b) and of 1.66 nm for device (c), in agreement with expected values. In the time domain the coherent superposition of two pulses at slightly different frequencies results in the beating modulation of temporal intensity, as sketched in Fig. 1(b). The measured autocorrelation traces [Fig. 2, curves (b) and (c)] exhibit oscillations with modulation depths smaller than 100%, as expected for a top-hat waveform with periodic dips whose widths are less than the separation between them.

The measured SH pulse energies of 180, 170, and 150 pJ for devices (a), (b), and (c), respectively, exhibit the expected efficiency scaling [Eq. (7)]. The peak spectral intensities are estimated as 760, 290, and 280 pJ/nm for devices (a), (b), and (c), respectively,

which are greater than the FH pulse peak spectral intensity of 270 pJ/nm.

In conclusion, we have demonstrated the use of QPM SHG spectral filtering for generation of dual-wavelength synchronous pulses. The demonstrated wavelength separation between pulses is limited by the FH pulse bandwidth but not by the technique itself. The nonlinear nature of such QPM SHG filtering allowed us to obtain spectral intensities at the SH higher than those at the FH. These devices are monolithic and compact and require no critical alignment. Future directions for research could include continuous tuning of the output by use of a fanlike grating,<sup>16</sup> use of waveguides for high efficiency at low pulse energies,<sup>17</sup> and obtaining larger wavelength separation between the SH pulses by use of a broader bandwidth source such as a sub-20-fs Ti:sapphire laser.

We thank Crystal Technology for a generous donation of lithium niobate wafers. This research was supported by U.S. Air Force Office of Scientific Research grant F49620-99-1-0270. M. M. Fejer's e-mail address is fejer@stanford.edu.

## References

1. M. R. X. de Barros and P. C. Becker, *Opt. Lett.* **18**, 631 (1993).
2. D. R. Dykaar, S. B. Darack, and W. H. Knox, *Opt. Lett.* **19**, 1058 (1994).
3. A. Leitenstorfer, C. Furst, and A. Laubereau, *Opt. Lett.* **20**, 916 (1995).
4. S. Wang, D. Xiao, J. Yang, S. Ruan, and X. Hou, *Proc. SPIE* **2869**, 527 (1997).
5. Y.-H. Chuang, Z.-W. Li, D. D. Meyerhofer, and A. Schmid, *Opt. Lett.* **16**, 7 (1991).
6. P. Langot, N. Del Fatti, R. Tommasi, and F. Vallee, *Opt. Commun.* **137**, 285 (1997).
7. M. A. Arbore, A. Galvanauskas, D. Harter, M. H. Chou, and M. M. Fejer, *Opt. Lett.* **22**, 1341 (1997).
8. G. Imeshev, A. Galvanauskas, D. Harter, M. A. Arbore, M. Proctor, and M. M. Fejer, *Opt. Lett.* **23**, 864 (1998).
9. M. A. Arbore, O. Marco, and M. M. Fejer, *Opt. Lett.* **22**, 865 (1997).
10. G. Imeshev, M. A. Arbore, M. M. Fejer, A. Galvanauskas, M. Fermann, and D. Harter, *J. Opt. Soc. Am. B* **17**, 304 (2000).
11. M. H. Chou, K. R. Parameswaran, M. M. Fejer, and I. Brener, *Opt. Lett.* **24**, 1157 (1999).
12. E. Sidick, A. Knoesen, and A. Dienes, *Pure Appl. Opt.* **5**, 709 (1996).
13. A. Knoesen, E. Sidick, and A. Dienes, in *Novel Optical Materials and Applications*, I.-C. Khoo, F. Simoni, and C. Umeton, eds. (Wiley, New York, 1997).
14. S. A. Akhmanov, V. A. Vysloukh, and A. S. Chirkin, *Optics of Femtosecond Laser Pulses* (American Institute of Physics, Melville, N.Y., 1992).
15. L. E. Myers, R. C. Eckardt, M. M. Fejer, R. L. Byer, W. R. Bosenberg, and J. W. Pierce, *J. Opt. Soc. Am. B* **12**, 2102 (1995).
16. P. E. Powers, T. J. Kulp, and S. E. Bisson, *Opt. Lett.* **23**, 159 (1998).
17. M. H. Chou, I. Brener, M. M. Fejer, E. E. Chaban, and S. B. Christman, *IEEE Photon. Technol. Lett.* **11**, 653 (1999).